RI bureau of mines
report of investigations 7407

EFFECTS OF EXPLOSIVE PROPERTIES ON FREE-SURFACE DISPLACEMENT PULSES AND CRATER DIMENSIONS

UNITED STATES DEPARTMENT OF THE INTERIOR

BUREAU OF MINES

July 1970

EFFECTS OF EXPLOSIVE PROPERTIES ON FREE-SURFACE DISPLACEMENT PULSES AND CRATER DIMENSIONS

By Richard L. Fischer, Dennis V. D'Andrea,
and David E. Fogelson

* * * * * * * * * * * * report of investigations 7407

UNITED STATES DEPARTMENT OF THE INTERIOR

BUREAU OF MINES

This publication has been cataloged as follows:

Fischer, Richard L

Effects of explosive properties on free-surface displacement pulses and crater dimensions, by Richard L. Fischer, Dennis V. D'Andrea, and David E. Fogelson. [Washington] U.S. Dept. of the Interior, Bureau of Mines [1970]

32 p. illus., tables. (U.S. Bureau of Mines. Report of investigations 7407)

Includes bibliography.

1. Explosives. I. D'Andrea, Dennis V., jt. auth. II. Fogelson, David E., jt. auth. III. Title. (Series)

TN23.U7 no. 7407 622.06173

U.S. Dept. of the Int. Library

CONTENTS

ILLUSTRATIONS

TABLES

EFFECTS OF EXPLOSIVE PROPERTIES ON FREE-SURFACE DISPLACEMENT PULSES AND CRATER DIMENSIONS

by

Richard L. Fischer,[1] Dennis V. D'Andrea,[2] and David E. Fogelson[3]

ABSTRACT

Constant-volume charges of precipitated PETN (pentaeythrite tetranitrate) at three specific gravities (0.50, 1.00, and 1.50) were used in laboratory tests to examine the effects of changes in explosive properties on free-surface displacement pulses and on crater dimensions. The tests were performed in large blocks of cement-mortar. The values for the detonation velocity, detonation pressure, specific energy, energy density, and energy release rate were calculated from the explosive loading density. Calculated explosive properties were correlated with free-surface displacement pulse measurements, strain energy, and measured crater dimensions. Increases in explosive properties resulted in increased free-surface displacement pulse parameters and crater dimensions. The loading density, detonation velocity, energy density, detonation pressure, and energy release rate were found to be best indicators of explosive performance. Simple acoustic relationships involving impedance ratios were examined and could not be used to predict peak displacement amplitude or strain energy. Data are presented in the customary English units as well as the International System of Units (SI).

INTRODUCTION

Rock breakage by chemical explosives is a complex process involving the physical properties of the rock mass, the detonation properties of the explosive, and blasting design conditions such as the hole spacing, loading, stemming, and initiation. General explosive and blasting information including safety aspects of storage, transportation, and use may be found in the Blaster's Handbook (12).[4] An information circular by Dick (7) contains information on explosive properties and explosive selection criteria plus some references of practical blasting techniques. Due to the complexity of the

---

[1] Research physicist.

[2] Geophysicist.

[3] Supervisory geophysicist.

All authors are with the Twin Cities Mining Research Center, Bureau of Mines, Minneapolis, Minn.

[4] Underlined numbers in parentheses refer to items in the list of references at the end of this report.

blasting problem selecting an explosive usually involves a judicious compromise between explosive performance economy (29) and blast design (1, 22) while giving proper consideration to application safety.

Explosive performance (without regard to economy) may be evaluated in several ways by standard testing methods (8, 24) such as the Trauzl lead block test and the ballistics pendulum test that are the bases for the strength ratings of commercial dynamites. Other methods of evaluating and comparing explosive performance include underwater pressure measurements (29), in situ linear array strain (3, 17, 27) pressure measurements in rock (5), and crater tests (10, 21, 30). Studies by the Bureau of Mines have shown that the measured amplitude and shape of the strain pulse are related to the size and shape of the craters produced in the rock (11).

This experiment was conducted as part of our continuing research program of studying the mechanisms of rock breakage and energy transfer. This report describes an experimental procedure used to evaluate the performance of an explosive in the laboratory. Explosive performance was evaluated by analyzing free-surface displacement pulse records from contained charges in cement-mortar and from crater tests with the same material and charges. Correlations were made between explosive properties and displacement pulse parameters, strain energy, and rock breakage by crater techniques. The strain energy was calculated from digitized free-surface displacement pulse records. The effect of impedance ratio on peak displacement and relative energy transmission for the simple acoustic case was examined. In these tests, PETN charges of small uniform grain size at three specific gravities (0.50, 1.00, or 1.50) were carefully fabricated to simulate explosives covering a wide energy range. The explosive properties were calculated from the chemical composition and the loading density with the aid of hydrodynamic detonation theory.

EXPLOSIVE DETONATION

Detonation in a high explosive charge is an extremely rapid, self-sustaining chemical reaction that produces a large volume of gas at a high temperature and a high pressure. To initiate detonation in a high explosive, both thermal energy and a shock process are required. Several authors, including Taylor (33), Eyring (13), Cook (6), and Dunkle (9), describe the detonation process according to the equation of hydrodynamic-thermodynamic theory. Hydrodynamic detonation theory is a complex subject that is not easily summarized. Yet the authors feel that a qualitative discussion of the detonation process is necessary to give the reader a better understanding of the explosive properties discussed in this report. The following discussion is taken largely from the above references.

Hydrodynamic detonation theory applies to explosive charges under complete confinement or of sufficient diameter to permit ignoring radial losses. The detonation properties describe the state of a chemical explosive following the passage of a steady-state, one-dimensional detonation wave. The following properties of the detonation zone may be calculated.

1. Detonation velocity.....D
2. Detonation pressure.....P
3. Detonation temperature.....T
4. Gas (particle) velocity.....W
5. Specific volume of detonation products.....V

From the known initial thermodynamic properties of the explosives these five unknown properties are determined by the simultaneous solution of five equations involving

1. Conservation of mass.
2. Conservation of energy.
3. Conservation of momentum.
4. Equation-of-state of the explosive.
5. The Chapman-Jouguet (CJ) condition.

The CJ condition specifies the minimum stable detonation velocity, D, that can exist in a detonating explosive column. Detonation is sonic with respect to the gaseous reaction products evaluated at the conditions of temperature, T, and density, 1/V, existing at the CJ plane:

$$D = W_{CJ} + C_{CJ} \tag{1}$$

where C_{CJ} = the velocity of sound in the gaseous products at the CJ plane

and W_{CJ} = the gas or particle velocity at the CJ plane.

The detonation velocity given by equation 1 is evaluated at the CJ plane. The exact position of the CJ plane is determined by conditions existing within the chemical reaction zone. For an ideal detonation--that is, one with a short reaction zone and corresponding small reaction time--the end of the chemical reaction zone coincides with the CJ plane. A nonideal detonation is generally associated with a longer reaction zone and the CJ plane is located within this zone. For this study detonations are assumed to be ideal.

Figure 1 diagrams a one-dimensional detonation wave in a column of PETN explosive. The detonation zone includes a thin shock zone, 10^{-5} cm, and a chemical reaction zone of the order of 0.1 cm. The shock zone is supported by a temperature-dependent chemical reaction zone. The detonation zone advances to the left at the explosive detonation velocity and the flow of the gaseous detonation products is toward the undetonated explosive.

Of the five detonation properties, the detonation velocity is the easiest to measure. The measurement techniques include photographic, continuous resistance wire, electronic time-interval methods, and the D'Autriche method (comparison of the unknown explosive velocity with the known velocity of detonating cord). The detonation velocity measurement gives a good indication of explosive performance. The peak detonation pressure at the end of the reaction zone is strongly influenced by the detonation velocity. Although the detonation pressure is an extremely important blasting parameter, it is not easily measured. Fortunately, however, it can be approximated from the detonation velocity and the loading density of the explosive.

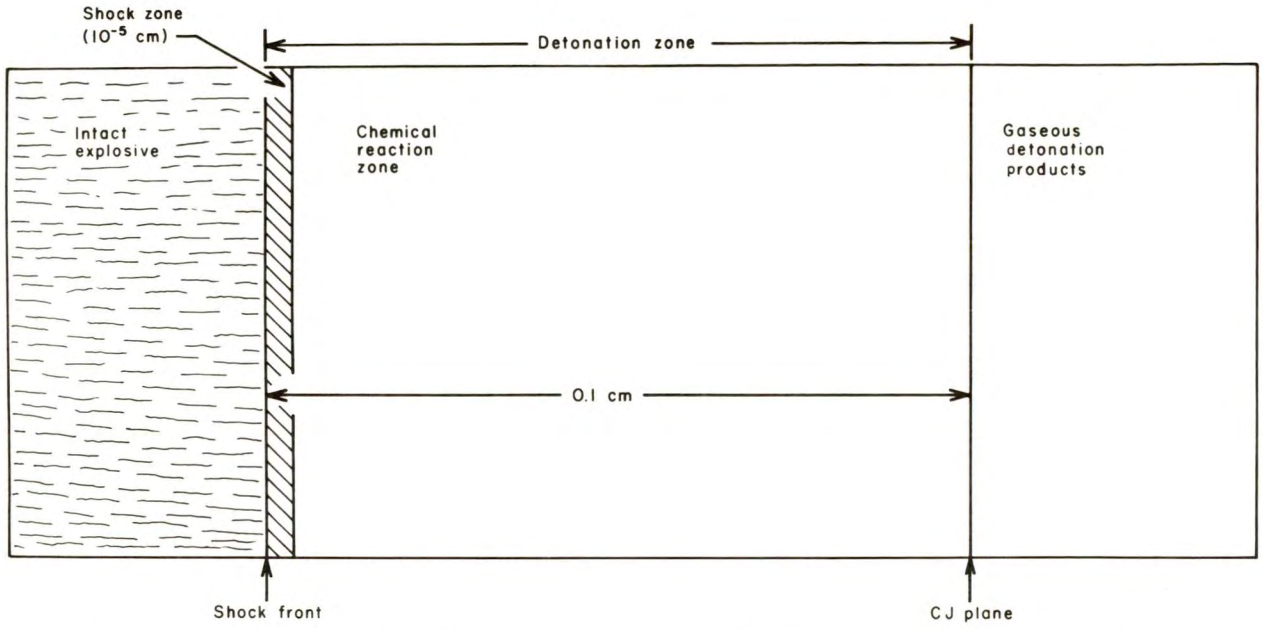

FIGURE 1. - Diagram of a Steady-State One-Dimensional Detonation Wave in PETN.

The detonation temperature cannot be measured directly but must be calculated from the products of detonation and an assumed equation-of-state. The equation-of-state of a substance is the relationship among the variables of pressure, volume or density, and temperature. When any two variables are known, the equation-of-state allows one to determine the unknown variable. The simplest equation-of-state for a gas is the well known ideal gas equation. Many more complex equations-of-state, which are beyond the scope of this report, introduce correction factors which bring the P-V-T relationships into better agreement with experimental data. The computed values of detonation temperature are strongly affected by the chosen equation-of-state, especially at the higher loading densities. Cook (6, p. 297) shows that detonation temperature is not only lower but decreases with loading density for some equations-of-state. When available, accurate experimental values of detonation temperature will enable researchers to determine the correct equation-of-state. The values of detonating temperature used in this report are taken from Brown (4).

EXPLOSIVE PROPERTIES

The charges used in these tests were prepared by R. Stressau Laboratory, Inc., Spooner, Wis., to specified specific gravities of 0.50, 1.00, and 1.50. The charges contained precipitated PETN as the main charge with lead azide as the initiating compound. Figure 2 is a schematic of the plastic-cased charge. Charge volumes were constant at 0.037 $in.^3$ (0.606×10^{-6} m^3) with length-to-diameter ratios of 3:1.

In these tests we attempted to simulate three different explosive types by varying the explosive loading density. Explosive properties such as

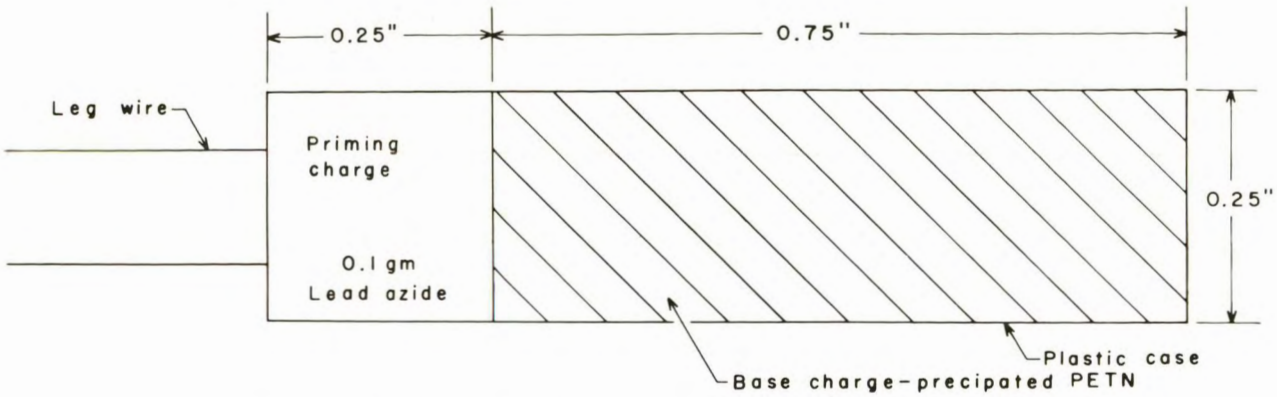

FIGURE 2. - Explosive Charge Diagram.

detonation velocity, detonation pressure, and energy density are dramatically affected by explosive density changes, while the detonation temperature and specific energy show little change. (See table 1 at the end of this section.)

The detonation velocity of most pure organic explosives such as PETN is a linear function of the specific gravity when the charge is properly initiated, well confined, and of adequate charge diameter. PETN is a sensitive explosive, having a short reaction zone length and a small critical diameter. The minimum explosive diameter (cylinder) that will support a stable detonation wave is defined as the critical diameter of the explosive. Ideal detonation is assumed for these tests. The detonation velocity for PETN can be approximated by the following empirical relationship:

$$D = a + b\rho \qquad (2)$$

where D = detonation velocity, ft/sec (m/sec)

and ρ = specific gravity.

For PETN: a = 5,250 (1 600) and b = 12,960 (3 950).

The detonation velocity is a sensitive indicator of explosive performance. In military explosives, the detonation velocity is the basis for quite accurate estimates of the detonation pressure, the energy liberated in the reaction, and the general effectiveness of the explosive (31). The detonation velocity is affected by several factors, such as the charge geometry, confinement, chemical composition, loading density, reaction zone width, particle size, and size distribution.

The effect of charge diameter and reaction zone width on detonation velocity for confined and unconfined charges has been investigated in the laboratory by Eyring and his associates (13), Cook (6), and others. Field studies on the effect of charge diameter on explosives performance were made by Nicholls and Duvall (26).

The effect of the explosive particle size and size distribution on the detonation velocity has been investigated for several explosive types. Tests (23) with explosives, such as ammonium picrate, indicate that compositions consisting of coarse particles have larger critical diameters than fine particle compositions. Certain mixtures of coarse and fine particles have even larger critical diameters with the maximum occurring at about 75 percent coarse material. The detonation velocity is similarly affected by explosive particle size and size distribution, with larger particle compositions detonating at lower velocities than smaller particles compositions and mixtures detonating at still lower velocities (31). The effects of particle size and size distribution are most pronounced in small-diameter charges of multicomponent explosives and tend to disappear with increasing charge diameter. Explosives containing uniformly small particle sizes detonate ideally in smaller diameters because explosive detonation is primarily a surface-eroding effect. To minimize particle size and size distribution effects, the charges used in these tests were carefully pressed from precipitated PETN.

Detonation pressure computations depend upon the equation-of-state selected. The isentropes given by the Jones and the Halford-Kistiakawsky-Wilson equations-of-state can be expressed by the gamma law equation (19) with gamma approximately equal to 3 in the detonation zone:

$$P/P_J = (\rho_E/\rho_{EJ})^{\gamma} \qquad (3)$$

where P = detonation pressure,

ρ_E = density (1/specific volume),

j = CJ value,

and γ = polytropic exponent (gamma).

This gamma should not be confused with the true ratio of specific heats, although it appears to play an analogous role in determining the detonation velocity. For $\gamma = 3$, the particle velocity $W = 1/4$, the detonation velocity D, equation 3 leads to the following expression involving the conservation equations in the detonation zone (9, p. 180):

$$P = K\rho_E D^2/4 \qquad (4)$$

where P = detonation pressure, psi (N/m^2),

ρ_E = density, lb/ft^3 (kg/m^3),

D = detonation velocity, ft/sec (m/sec),

and K = constant depending on units, 2.16×10^{-4} (10^{-8}).

Like the equations based on more complex equations-of-state, equation 4 will approximate the actual density-pressure relationships in an explosive detonation. The use of equation 4 simplifies computation and yields overall satisfactory results. Jacobs (19) summarized the findings of many investigators

and concluded that irrespective of the methods of approach, most calculations of detonation pressure fall into a range of about ±10 percent. Better results require equation-of-state parameters normalized to the experimental data.

A measure of the relative energy of an explosive may be obtained by calculating its ballistic mortar parameter or specific energy. The specific energy is sometimes erroneously called "strength," "power," or "explosive force," though it is expressed in units of heat or energy rather than force or power. Specific energy, B, usually expressed in calories per gram or foot-pound (kJ/kg) is determined as follows:

$$B = NRT \text{ cal/g} \tag{5}$$

where N = specific gas volume of the reaction product (0.0352 mole/g for PETN),

R = universal gas constant, 1.987 g cal/(g mole) (° K),

and T = detonation temperature, ° K.

This calculated energy is about the same as the ballistic mortar test energy which is calculated from the recoil of a pendulum system. Brown (4) states that the lead-block test results can also be correlated with ballistic mortar tests and specific energy.

For the purposes of this experiment it is useful to multiply the specific energy by the explosive density, ρ_E.

$$E = B\rho_E \tag{6}$$

where E = energy density, ft lb/ft^3 (J/m^2),

B = specific energy, ft lb/lb (kJ/kg),

and ρ_E = density, lb/ft^3 (kg/m^3).

This quantity, designated as the explosive energy density, is an expression of explosive energy per unit volume. Because energy density is calculated on a volume rather than a weight basis, it is a useful term for discussing and comparing the experimental results of this report and field results in drill holes of constant size. Its practical value stems from the fact that it is a composite calculation involving specific energy and loading density. Either specific energy or loading density alone may not give a true picture of explosive performance. While specific energy is approximately independent of loading density, the energy density of PETN is approximately a linear function of the loading density.

The explosive energy release rate is a measure of explosive intensity or power. Its usefulness includes comparing different forms of energy such as explosive with electrical or thermal energy. The energy release rate is defined as

$$I = ED \tag{7}$$

where I = energy release rate, ft lb/ft^2 sec (W/m^2),

E = energy density, ft lb/ft^3 (J/m^3),

and D = detonation velocity, ft/sec (m/sec).

The full implications of this explosive parameter require further investigation. It can be controlled by varying the explosive composition, explosive density, the size of the initiating charge or the number of simultaneous initiation points. With point charges, this parameter has little significance but with cylindrical charges, Starfield and Pugliese (32) note that computer simulated strain waveforms are largely dependent upon the superposition of incremental wavelets--that is, incremental bursts of energy occurring at the detonation rate of the explosive.

Table 1 lists the explosive properties of PETN at three loading densities and the explosive-to-medium impedance ratio. The characteristic impedance of the concrete mortar is 34.6 lb sec/in^3 (9.38 MN sec/m^3), where the impedance is the product of the density and the longitudinal propagation velocity.

TABLE 1. - Explosive properties of PETN

Specific gravity, ρ	0.50	1.00	1.50
Density, ρ_E[1]	31.2	62.4	93.6
lb/ft^3 (kg/m^3)	(500)	(1,000)	(1,500)
Detonation velocity, D	11.7	18.2	24.7
10^3 ft/sec (m/sec)	(3,580)	(5,550)	(7,520)
Detonation pressure, P	0.232	1.12	3.09
10^6 psi (GN/m^2)	(1.61)	(7.70)	(21.2)
Detonation temperature, $^\circ$ K[2]	5,000	5,140	5,340
Specific energy, B	0.489	0.504	0.522
10^6 ft lb/lb (kJ/kg)	(1.46)	(1.51)	(1.56)
[k cal/kg]	[349]	[359]	[373]
Energy density, E	15.3	31.4	48.9
10^6 ft lb/ft^3 (GJ/m^3)	(0.730)	(1.51)	(2.34)
Energy release rate, I	0.18	0.57	1.20
10^{12} ft lb/ft^2 sec (TW/m^2)	(2.61)	(8.38)	(17.6)
Characteristic impedance, $\rho_E D$	6.60	20.4	41.6
[3] lb sec/in^3 (MN sec/m^3)	(1.79)	(5.55)	(11.3)
Impedance ratio, R[4]	0.191	0.591	1.20

[1] Weight density in English units; mass density in SI units.
[2] Values obtained from F. W. Brown (4).
[3] 5.6×10^{-4} $\rho_E D/g$ (English units) where g = 32.2 ft/sec^2.
[4] R = $\rho_E D$ (explosive)/$\rho_M C$ (medium).

PHYSICAL PROPERTIES OF CEMENT-MORTAR

All tests discussed in this report were performed in blocks of water-cured, high-strength cement-mortar of similar composition.

The composition of the 30 by 30 by 60 in. blocks was 2 parts of sand to 1 part of regular portland cement and sufficient water to make a 2-in. slump (about 30 gal/yd^3). The largest grain contained in the mix was 5/16 in. and particle size distribution of the cement-mortar mixture is shown in table 2.

TABLE 2. - Particle size distribution in cement-mortar mixture[1]

	Weight-percent
Plus 8 mesh	15
Minus 8 plus 28 mesh	52
Minus 28 plus 100 mesh	29
Minus 100 mesh	4

[1]Specific gravity, 2.71; composition, mainly quartz and feldspar.

Table 3 lists the results of physical property tests on the cement-mortar cores using published laboratory testing procedures (21). The pull-tensile strength test is described by Fairhurst (14).

TABLE 3. - Physical properties of cement-mortar mixture

Number of tests	Physical property	Mean value	Standard deviation
11	Compressive strength, psi	7,800	1,000
	(MN/m^2)	(53.8)	(6.89)
9	Tensile strength, psi	480	70
	(MN/m^2)	(3.31)	(0.48)
7	Longitudinal pulse velocity, ft/sec	14,400	10
	(m/sec)	(4,390)	(3)
7	Torsional velocity, ft/sec	8,030	20
	(m/sec)	(2,450)	(6)
7	Bar velocity, ft/sec	12,700	80
	(m/sec)	(3,870)	(24)
6	Young's modulus (static), 10^6 psi	2.6	0.2
	(GN/m^2)	(17.9)	(0.38)
5	Density, ρ_M[1]	134	(0.7)
	lb/ft^3 (kg/m^3)	(2,140)	(10)

[1]Weight density in English units; mass density in SI units.

EXPERIMENTAL PROCEDURE

Displacement Pulse Measurements

For the free-surface displacement pulse measurements, a charge was detonated at the bottom of a drill hole in a cement-mortar block and the resulting pulse was recorded by two capacitive displacement gages placed on opposite

sides of the block. These tests employed capacitive type gages because available commercial transducers will not respond to the high frequencies generated by these small explosive charges. As shown in figure 3 the shotholes were 10 in. deep and spaced about 6 in. apart along the 60 in. block. A new shothole was drilled for each test to avoid any effects of repeat shooting. To eliminate bias, the different charge densities were detonated in random order. The shot-to-gage distance of 15 in. remained constant for each shot. For each charge density two shots were fired and produced four displacement-time records.

Figure 4 is a diagram of a typical shothole showing the position of the charge. The unusual hole geometry is a result of the difficulty of drilling small-diameter holes to a depth of 10 in. with a rotary-percussive drill. The drilling procedure consisted of drilling a 1-in. diameter hole to a depth of about 8 in. and then using an extension with a 5/16-in. bit for drilling the remaining portion. The effective diameter of the shothole was 5/16 in., as all shots were fired in this portion of the shothole. Although the charges were only 80 percent coupled (ratio of charge diameter to hole diameter to the cement-mortar), this effect was somewhat lessened by stemming with fine silica sand.

The free-surface displacement pulses were measured with a capacitive displacement gage. The experimental technique and equipment are described in an earlier report (15). The system consists of two capacitive displacement gages,

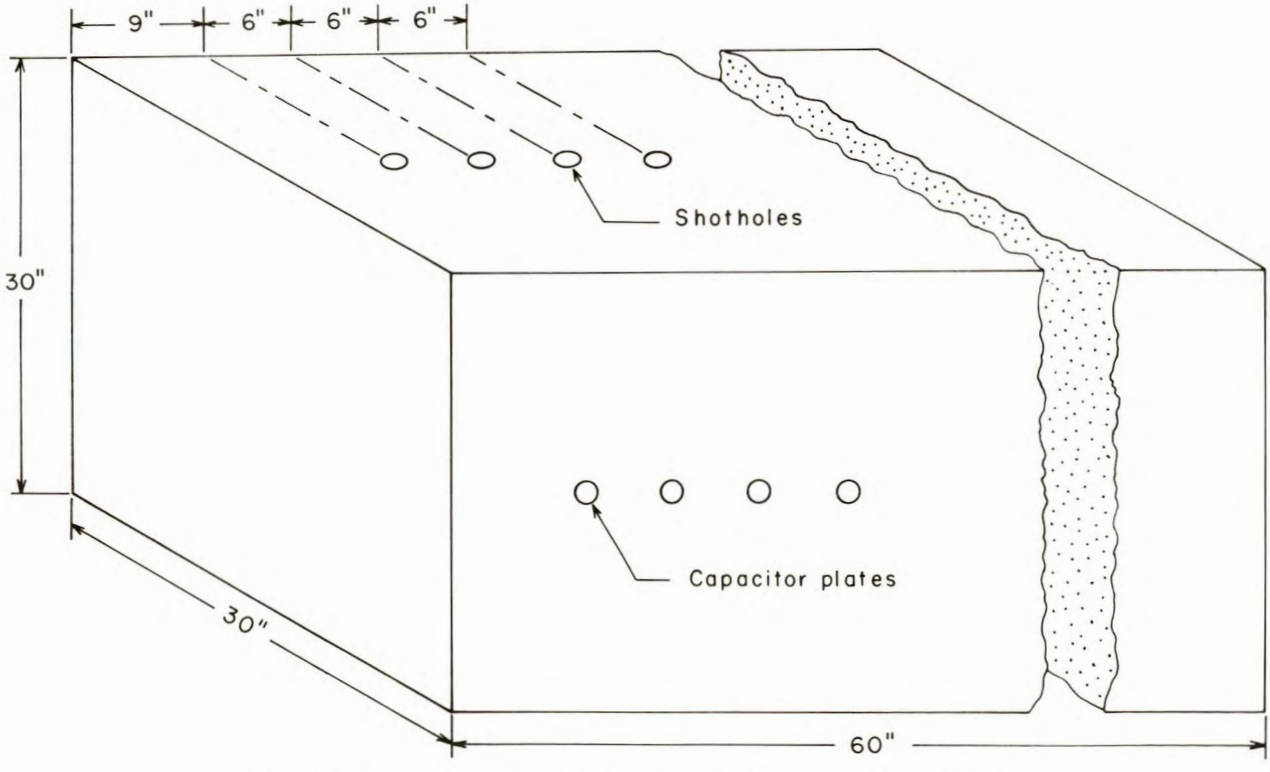

FIGURE 3. - Location of Shotholes in Cement-Mortar Block.

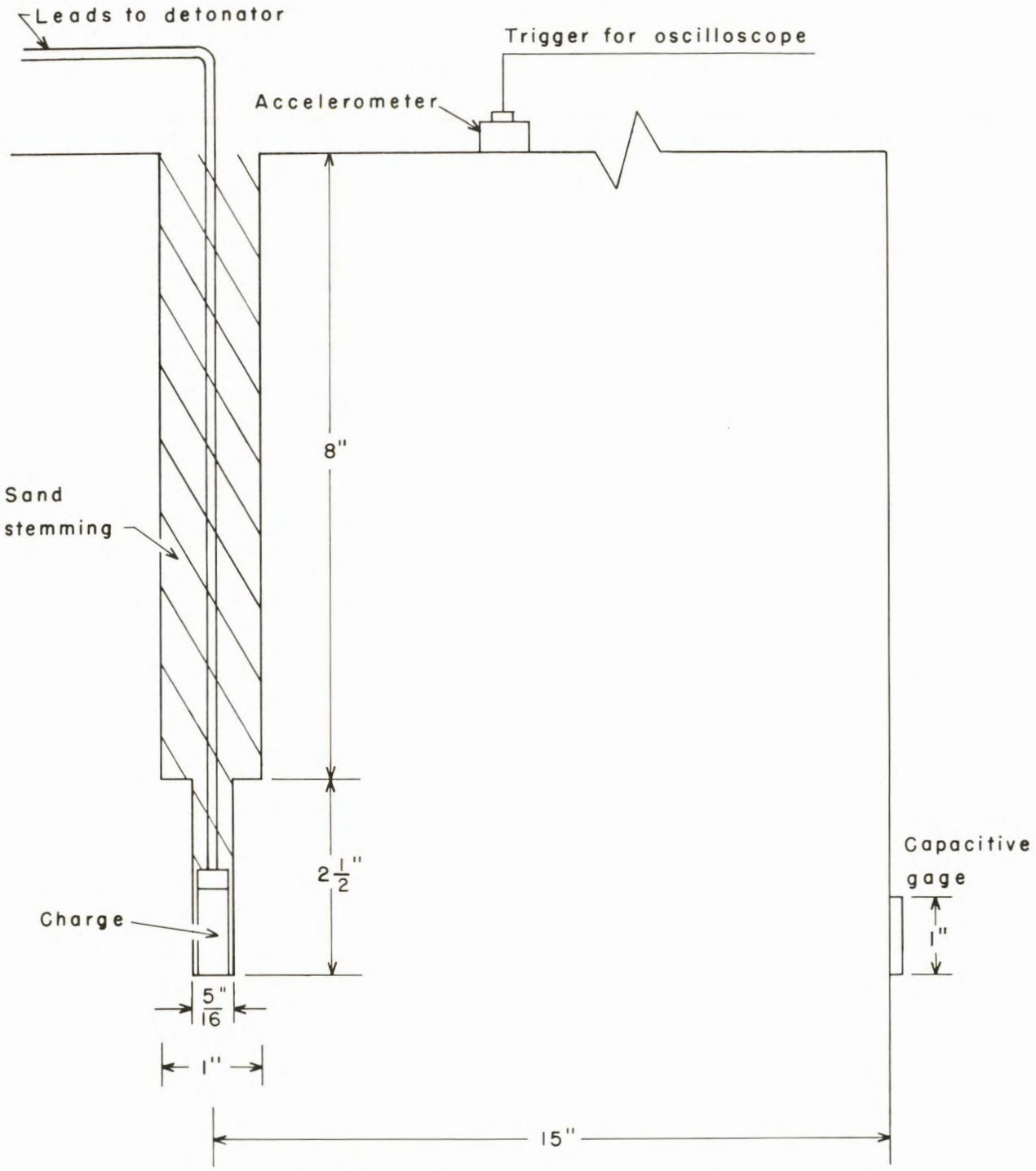

FIGURE 4. - Diagram of Charge in Shothole.

two feed units, a battery power supply, a triggering device, and an oscilloscope with attached camera.

The oscilloscope triggering device used in these tests was an accelerometer rather than an ionization probe. The surface-mounted accelerometer (fig. 4) proved to be a reliable and useful device. Positioned to provide delay in the trigger circuit, the accelerometer thus permitted the use of the single sweep operation at a faster sweep rate. A faster oscilloscope sweep rate gives better pulse definition and permits more accurate measurement of pulse parameters.

The circuit diagram of a capacitive gage is shown in figure 5. For small displacement, the free-surface displacement is given by the following equation:

$$\Delta X = (\Delta V/V)\,(C_1 + C_g)\,X/C_g \qquad (8)$$

where ΔX = free-surface displacement,

ΔV = measured voltage amplitude on photographed oscilloscope trace,

V = battery supply voltage,

C_1 = capacitance of feed unit circuit,

C_g = gage capacitance,

and X = gage plate separation.

The capacitive gage will respond to very high frequency wave motion and its high frequency response is limited by the bandwidth of the oscilloscope amplifier.

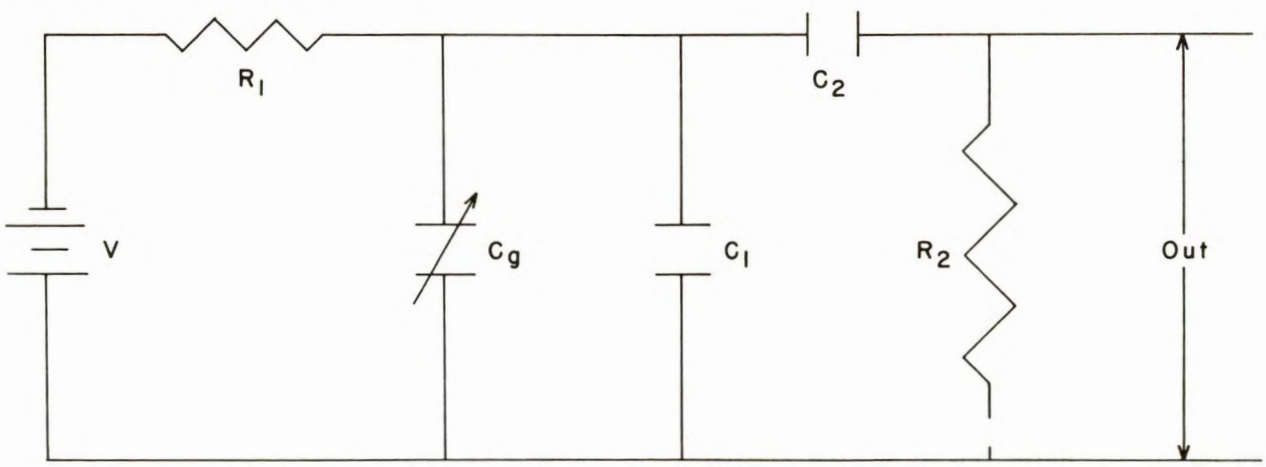

V = 480 volts
R_1 = 45 megohms
C_g = Gage capacitance
C_1 = 0.001 microfarad
C_2 = 0.1 microfarad
R_2 = 2 megohms

FIGURE 5. - Feed-Unit Circuit.

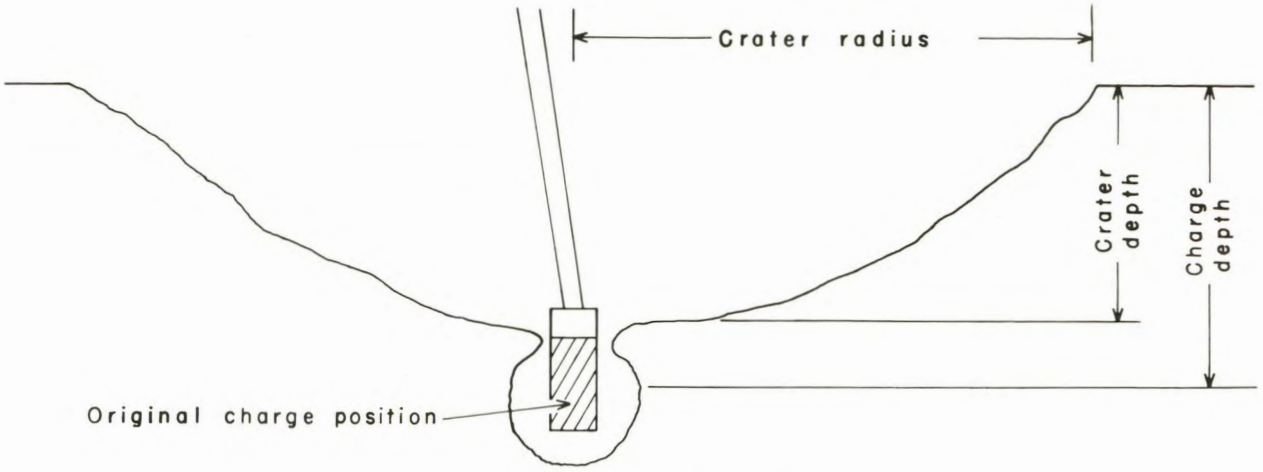

FIGURE 6. - Typical Crater.

Crater Tests

Using established laboratory techniques (20-21), crater tests were performed with similar PETN charges of the three specific gravities. For each test, a charge was placed in the bottom of a shothole 5/16 in. in diameter and stemmed to the collar with fine dry sand. The charge depth was measured from the center of the base charge--that is, the hole depth less 3/8 in. After detonation, the resulting crater depth, crater radius, and crater volume were measured. The volume measurement was made by filling the crater with a measured volume of dry silica sand. Figure 6 illustrates how the length dimensions were measured in a typical crater.

EXPERIMENTAL DATA

Displacement Pulse Data

The displacement data consist of 12 equidistant free-surface displacement pulse recordings. There are two recordings for each shot. Figure 7 is an example of three typical shot records. Initially, the trace is at zero amplitude with time after triggering increasing from left to right. Trace deflections below the baseline represent the outward free-surface displacements resulting from an explosion-generated compressive pulse.

Figure 8 is an idealized diagram of a free-surface displacement pulse. In accordance with proposed standards (18), all pulse parameters except duration were defined from the peak amplitude--the least ambiguous pulse measurement. These definitions are based upon the geometry of the individual static pulse and are independent of frequency and application.

Table 4 lists the free-surface displacement pulse measurements for the three charge types. The measurements listed are peak amplitude, duration, width, rise time, and fall time.

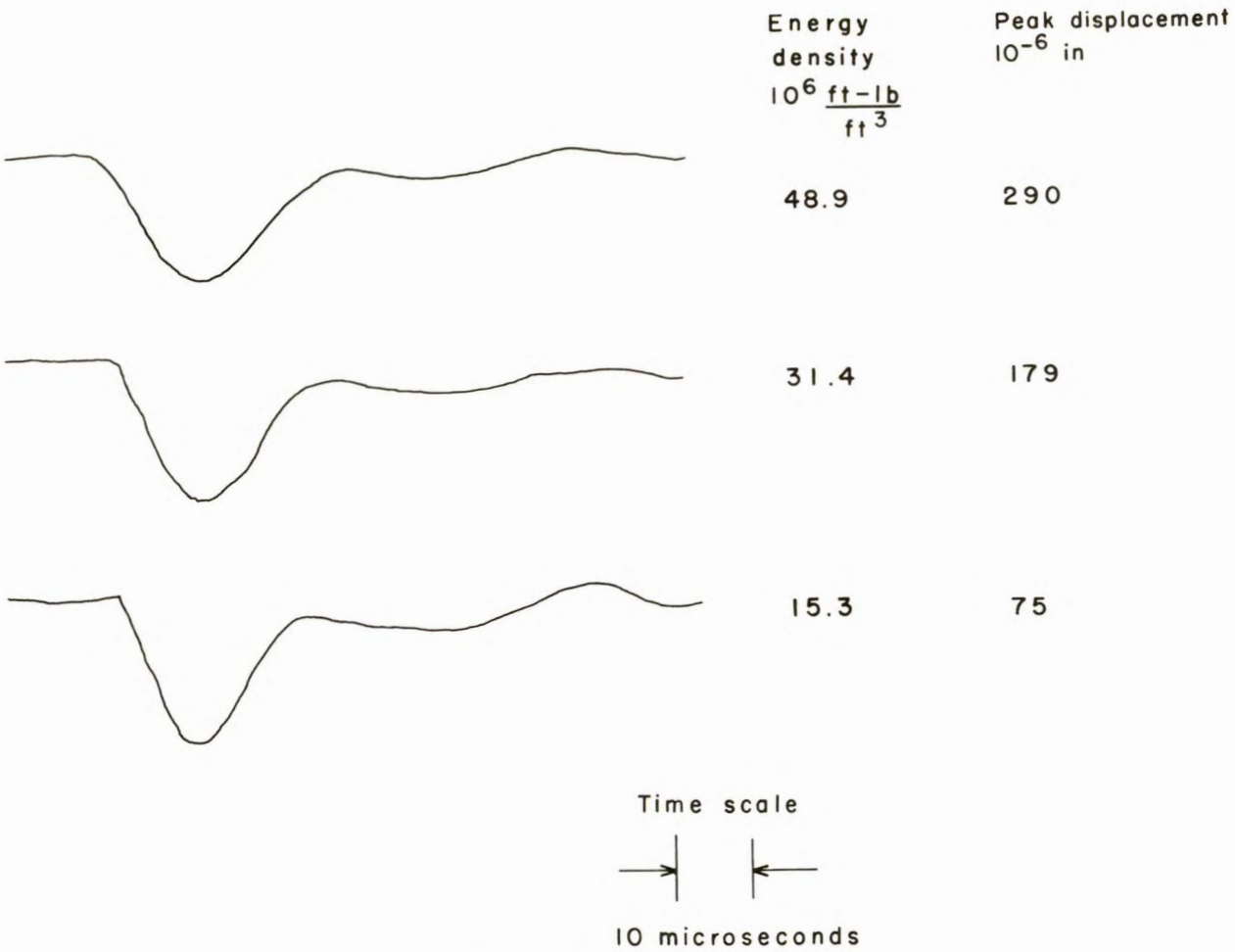

FIGURE 7. - Typical Shot Records.

TABLE 4. - Displacement pulse measurements

ρ	Pulse parameters				
	Amplitude 10^{-6} in. (μm)	Duration 10^{-6} sec	Rise time 10^{-6} sec	Fall time 10^{-6} sec	Pulse width 10^{-6} sec
0.50	67 (1.70)	25	7.5	8.0	13.0
	73 (1.85)	25	7.5	7.0	12.0
	75 (1.90)	24	8.5	9.0	13.0
	77 (1.96)	25	8.0	8.0	13.0
1.00	179 (4.55)	28	10.0	9.0	16.0
	145 (3.68)	32	10.0	10.0	17.0
	165 (4.19)	31	9.0	10.0	17.0
	181 (4.60)	29	10.0	10.5	16.0
1.50	290 (7.37)	33	12.0	12.0	19.0
	217 (5.51)	34	11.0	10.0	19.0
	254 (6.45)	35	11.0	11.0	19.0
	271 (6.88)	36	11.0	11.0	19.0

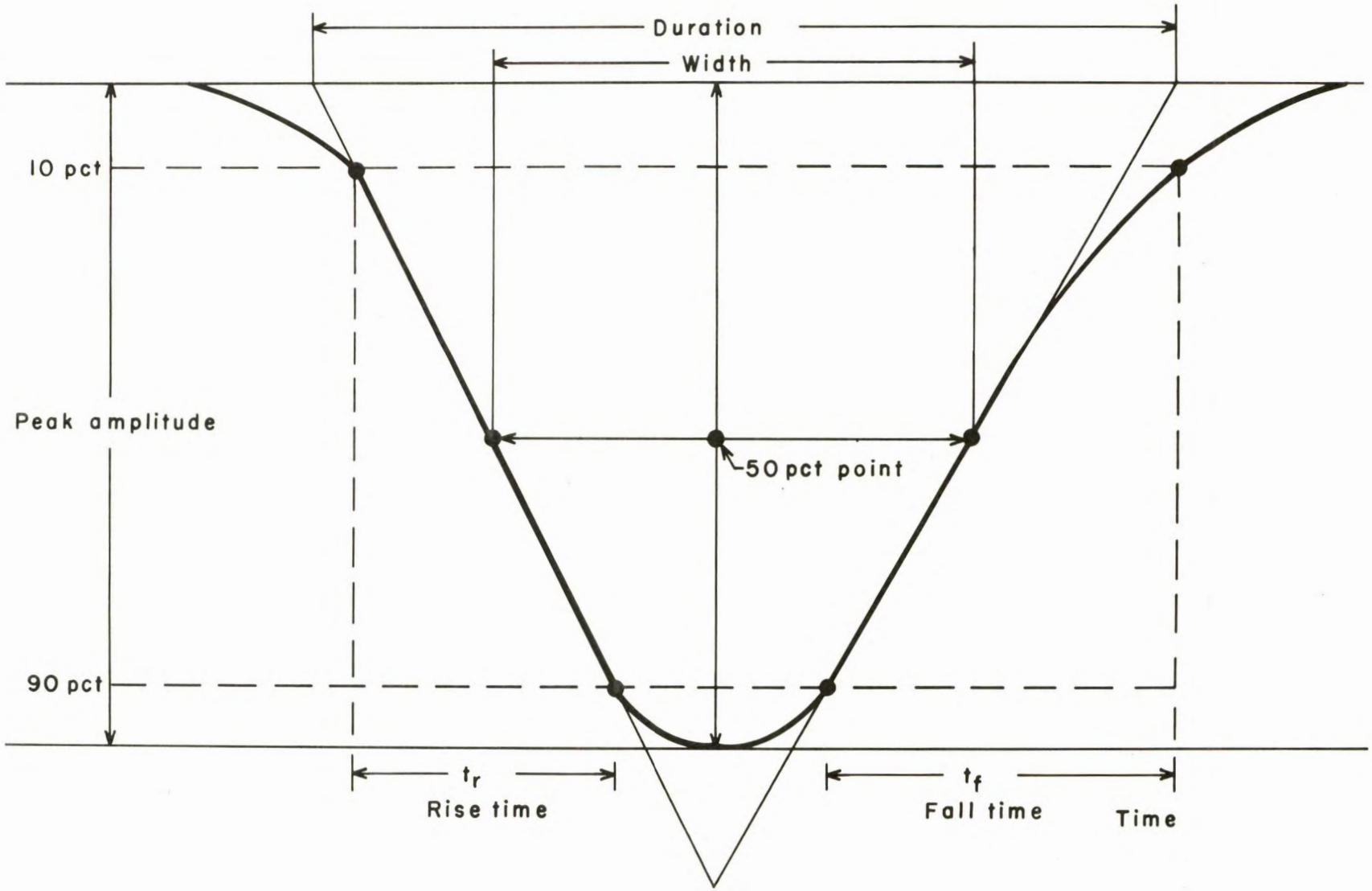

FIGURE 8. - Displacement Pulse Measurements.

Crater Data

The crater test data for the laboratory-scale tests are presented in table 5. For each charge type, measurements of crater depth, radius, and volume are given at several charge depths. The burial depth of the explosive charge was varied to provide sufficient points for defining the crater curves.

TABLE 5. - Crater data

ρ	Hole depth in. (mm)	Crater depth in. (mm)	Crater radius in. (mm)	Crater volume in.^{3} (μm^3)	Charge depth in. (mm)
0.50	1.0 (25.4)	0.292 (7.41)	1.25 (31.8)	0.49 (8)	0.625 (15.9)
	1.18 (30.0)	.41 (10.4)	1.28 (32.5)	1.10 (18)	.805 (20.4)
	1.33 (33.8)	.47 (11.9)	1.25 (31.8)	1.10 (18)	.955 (24.3)
	1.50 (38.1)	.344 (8.73)	2.25 (57.2)	3.66 (60)	1.125 (28.6)
	1.70 (43.2)	.312 (7.92)	1.10 (27.9)	.43 (7)	1.325 (33.7)
	1.87 (47.5)	.56 (14.2)	1.68 (42.7)	1.83 (30)	1.495 (38.0)
	2.0 (50.8)	.219 (5.56)	.75 (19.0)	.18 (3)	1.625 (41.3)
1.00	1.0 (25.4)	.531 (13.5)	1.44 (36.6)	1.83 (30)	.625 (15.9)
	1.25 (31.8)	.594 (15.1)	2.36 (59.9)	4.39 (72)	.875 (22.2)
	1.50 (38.1)	.750 (19.0)	2.94 (74.7)	5.98 (98)	1.125 (28.6)
	1.75 (44.4)	.845 (21.5)	2.75 (69.8)	6.90 (113)	1.375 (34.9)
	2.0 (50.8)	.875 (22.2)	2.72 (69.1)	6.71 (110)	1.625 (41.3)
	2.31 (58.7)	1.94 (49.3)	3.55 (90.2)	14.0 (230)	1.935 (49.1)
	2.50 (63.5)	[1] [1]	[1] [1]	[1] [1]	2.125 (54.0)
1.50	1.0 (25.4)	.655 (16.6)	1.44 (36.6)	3.66 (60)	.625 (15.9)
	1.5 (38.1)	.813 (20.6)	3.11 (79.0)	9.46 (155)	1.125 (28.6)
	2.0 (50.8)	1.312 (33.3)	5.5 (140)	35.6 (584)	1.625 (41.3)
	2.5 (63.5)	1.094 (27.8)	4.1 (104)	14.8 (242)	2.125 (54.0)
	3.0 (76.2)	1.906 (48.4)	6.6 (168)	58.8 (963)	2.625 (66.7)
	3.5 (88.9)	[1] [1]	[1] [1]	[1] [1]	3.125 (79.4)

[1] No crater.

DATA ANALYSIS

Peak Displacement

The data were first analyzed (28) to determine the effects of explosive properties on the peak amplitude of free-surface displacement pulses. Figure 9 shows peak displacement as a function of the explosive properties. The method of least squares was used to fit the curves or lines through the data shown in figure 9. Peak displacement increases as the values of all explosive properties increase as shown in figure 9. There is a linear relationship between peak displacement and explosive loading density, detonation velocity, specific energy, and energy density. The relationship between peak displacement and detonation pressure or energy release rate is nonlinear.

There are large changes in peak displacement associated with small percentage changes in specific energy. Peak displacement, however, is nearly

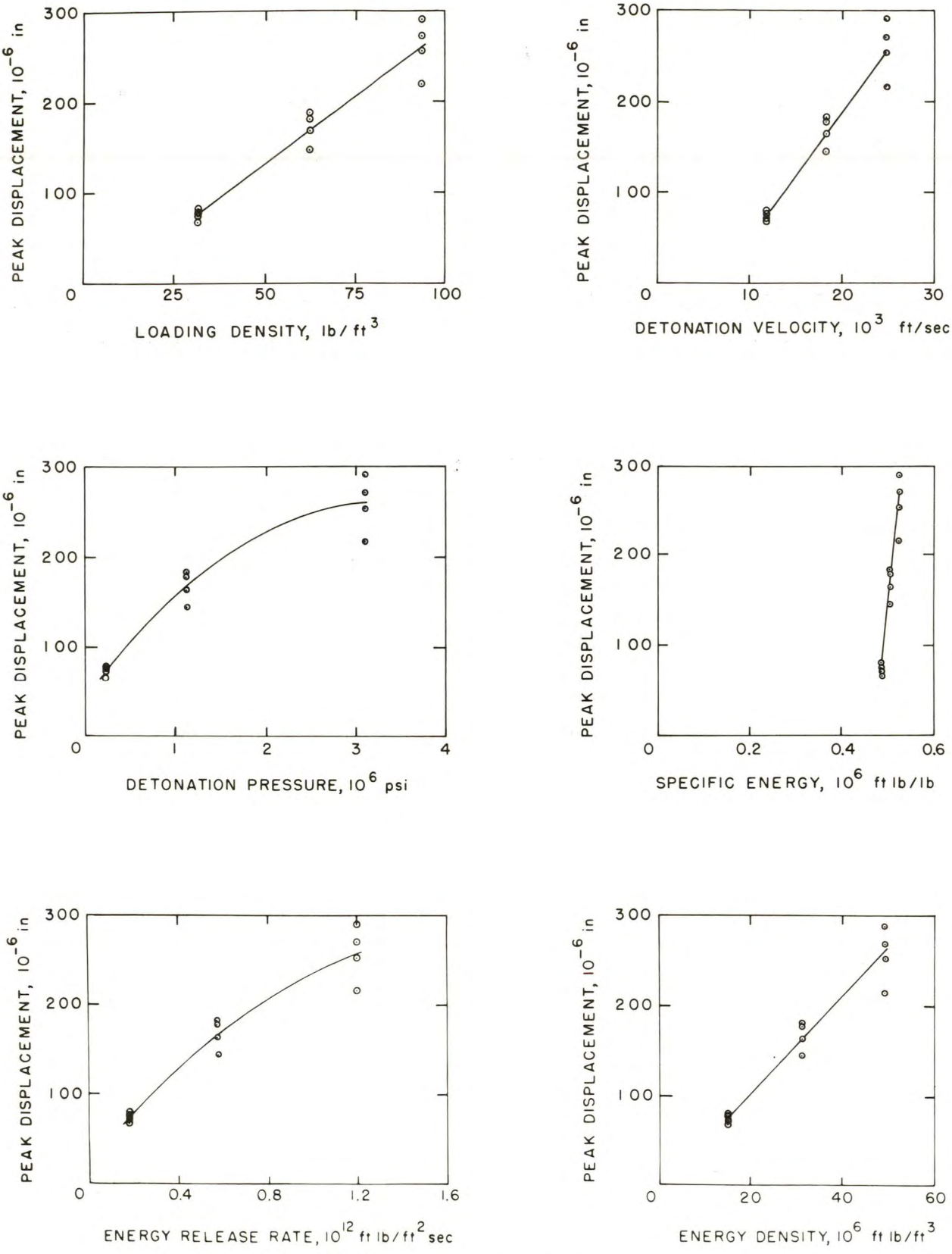

FIGURE 9. - Peak Displacement as a Function of Explosive Properties.

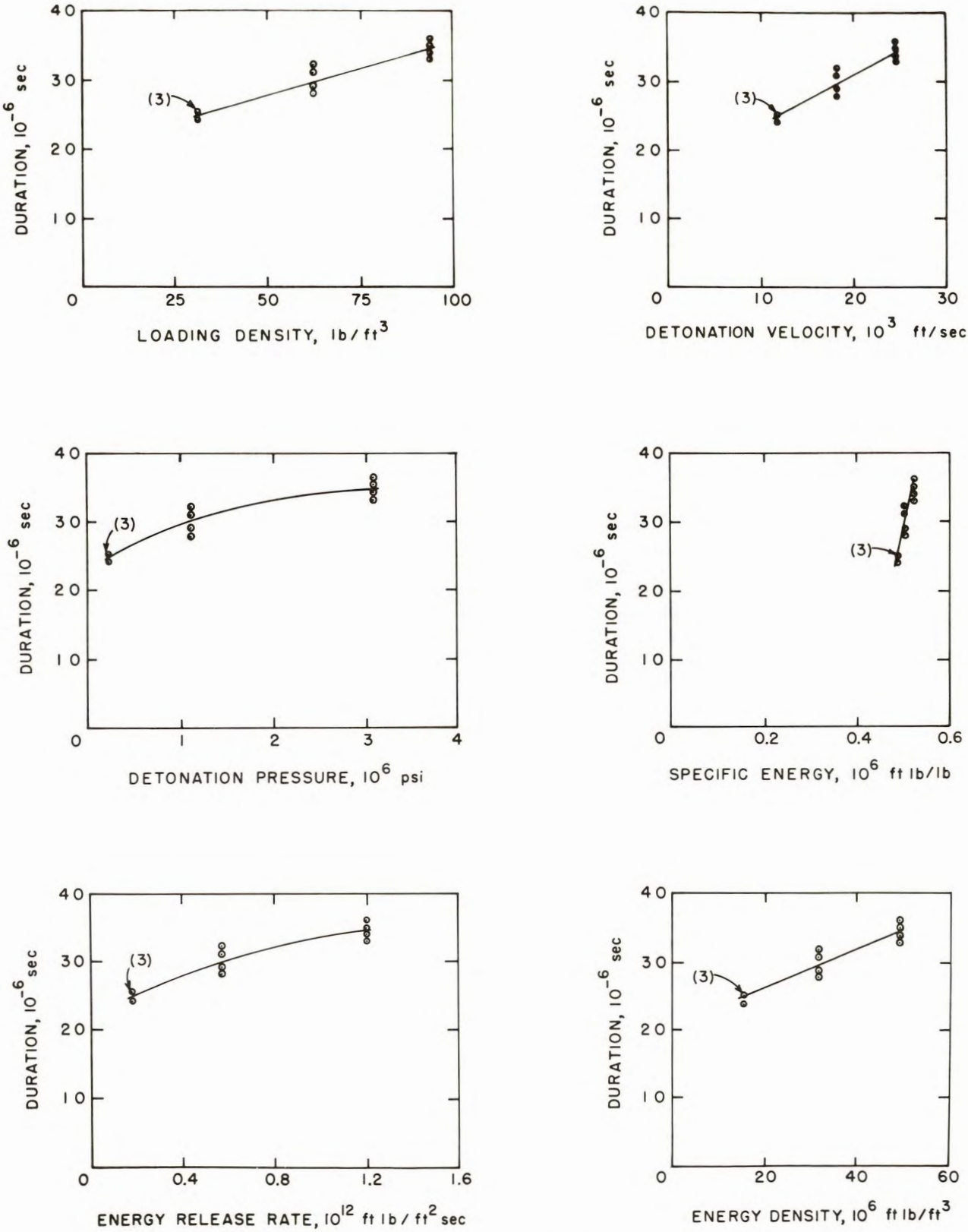

FIGURE 10. - Displacement Pulse Duration as a Function of Explosive Properties.

directly proportional to energy density, suggesting that energy density is a better indicator of explosive performance than specific energy.

Displacement Pulse Duration

Figure 10 shows free-surface displacement pulse duration as a function of the explosive properties. Free-surface displacement pulse duration increases with increasing values of the explosive properties. The percentage increase in duration is not as large as the percentage increase in peak displacement. In figure 10 the plots of loading density, detonation velocity, specific energy, and energy density show linear relationships. The relationship between displacement pulse duration and detonation pressure or energy release rate is nonlinear.

Changes in displacement pulse rise time, fall time, and width with increasing values of explosive properties are similar to the changes observed for displacement pulse duration.

Strain Energy

The radial strain energy, E_s, was calculated from the observed displacement pulses by the strain energy equation given by Fogelson (16):

$$E_s = 2\pi R^2 \rho_M C^3 \int_0^t \epsilon_r^2 \, dt \tag{9}$$

where ρ_M = density of cement-mortar,

R = shot distance,

C = longitudinal velocity of cement-mortar,

ϵ_r = radial strain,

and t = time.

The radial strain, ϵ_r, was calculated from the plane wave relationship

$$\epsilon_r = (1/2c)(\partial d/\partial t) \tag{10}$$

where d = free-surface displacement.

Combining equations 9 and 10, the radial strain energy in the wavefront at the distance R from the explosive source is given by

$$E_s = \pi R^2 \rho_M C/2 \int_0^t (\partial d/\partial t)^2 \, dt. \tag{11}$$

The displacement records were digitized and computer programs were written to perform the operations indicated in equation 11. The values of radial strain energy for the three charge types are listed in table 6. The

free-surface displacement pulses were measured at a distance of 15 in. from the explosive source. The strain energy values listed in table 6 will be lower than the actual energy transferred to the cement-mortar because of energy absorption in this first 15 in.

TABLE 6. - Peak displacement and strain energy[1]

ρ	Peak displacement 10^{-6} in. (μm)	Strain energy ft lb (J)
0.50	67 (1.70)	0.83 (1.13)
.50	73 (1.85)	.97 (1.32)
.50	75 (1.90)	1.09 (1.48)
.50	77 (1.96)	1.15 (1.56)
Average	73 (1.85)	1.01 (1.37)
1.00	179 (4.55)	4.8 (6.51)
1.00	145 (3.68)	2.5 (3.39)
1.00	165 (4.19)	3.8 (5.15)
1.00	181 (4.60)	5.0 (6.78)
Average	168 (4.27)	4.02 (5.45)
1.50	290 (7.37)	10.4 (14.1)
1.50	217 (5.51)	5.7 (7.73)
1.50	254 (6.45)	8.4 (11.4)
1.50	271 (6.88)	11.7 (15.9)
Average	258 (6.55)	9.05 (12.3)

[1]Recorded at 15 in. from explosive charge.

Figure 11 shows strain energy as a function of the explosive properties. There is a linear relationship between strain energy and detonation pressure, specific energy, and energy release rate. The relationship between strain energy and loading density, detonation velocity, and energy density is nonlinear.

The strain energy is not directly proportional to the specific energy or the energy density. The transfer of energy from the explosive to the rock then is more complex than a simple 1:1 relationship.

Characteristic Impedance Effects

For a plane elastic wave striking a plane boundary at normal incidence the transmitted pressure, P_t, and the incident pressure, P_i, are related by

$$P_t/P_i = 2/(1 + R) \tag{12}$$

where R = characteristic impedance ratio.

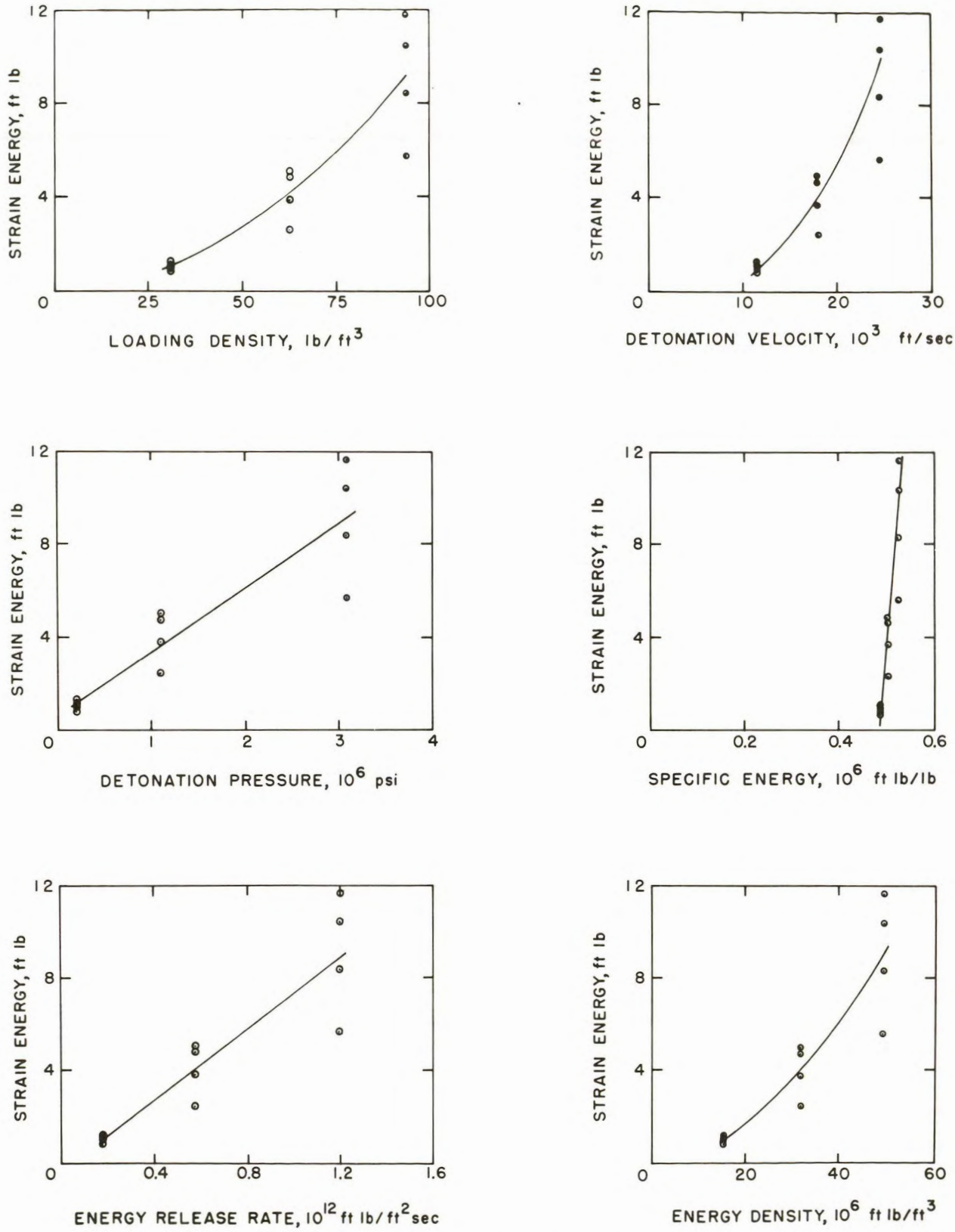

FIGURE 11. - Strain Energy as a Function of Explosive Properties.

If it is assumed that P_i is the detonation pressure of an explosive, P_t is the stress in the medium and R is the ratio of the characteristic impedance of the explosive to that of the rock, it can be shown that the peak strain, detonation pressure of the explosive, and characteristic impedance ratio are related (25) by

$$K/P = A/2(1 + R) \tag{13}$$

where K = peak strain at unity scaled distance,

P = detonation pressure,

and A = a constant.

It has been shown experimentally that equation 13 does not describe observed phenomena. However, empirical correlations between peak amplitudes of wave motions divided by detonation pressure and characteristic impedance have been observed (25). In all cases the impedance effect is larger than that predicted by the simple acoustic predictions of equation 13. Figure 12 shows peak displacement divided by detonation pressure plotted against characteristic impedance ratio for the data in this report. The dashed line is the simple acoustic case and is shown here also to not accurately describe the observations. The dashed line is drawn to intersect the line through the experimental data at R = 1.

For the acoustic case, energy is transmitted according to the following expression (2):

$$E_t/E_i = 4r/(1 + R)^2 \tag{14}$$

where E_t = transmitted energy

and E_i = incident energy.

Empirical relationships of the form given by equation 14 have been found to fit experimental data reasonably well when the scaled strain energy is divided by the energy density of the explosive and plotted against characteristic impedance ratio (2). Figure 13 shows the relative energy transfer as a function of characteristic impedance ratio for the data in this report. The relative energy is the scaled strain energy from table 6 divided by the explosive energy density. Volume scaling produces no relative change in the strain values. The explosive-to-medium impedance ratio ranged from 0.19 to 1.2 for these tests. The dashed line in this figure represents the simple acoustic case and is drawn to intersect the least squares line through the data at R = 1. Figure 13 shows that for these data the increase in relative energy transfer with increasing impedance ratio is larger than that predicted by the simple acoustic case. Also the acoustic case predicts that energy transfer will be most efficient when the impedance of the explosive equals the impedance of the rock. The data shown in figure 13 suggest that energy transfer continues to be increasingly efficient beyond impedance ratios of 1.0. More data of the high impedance ratios are required to confirm this finding.

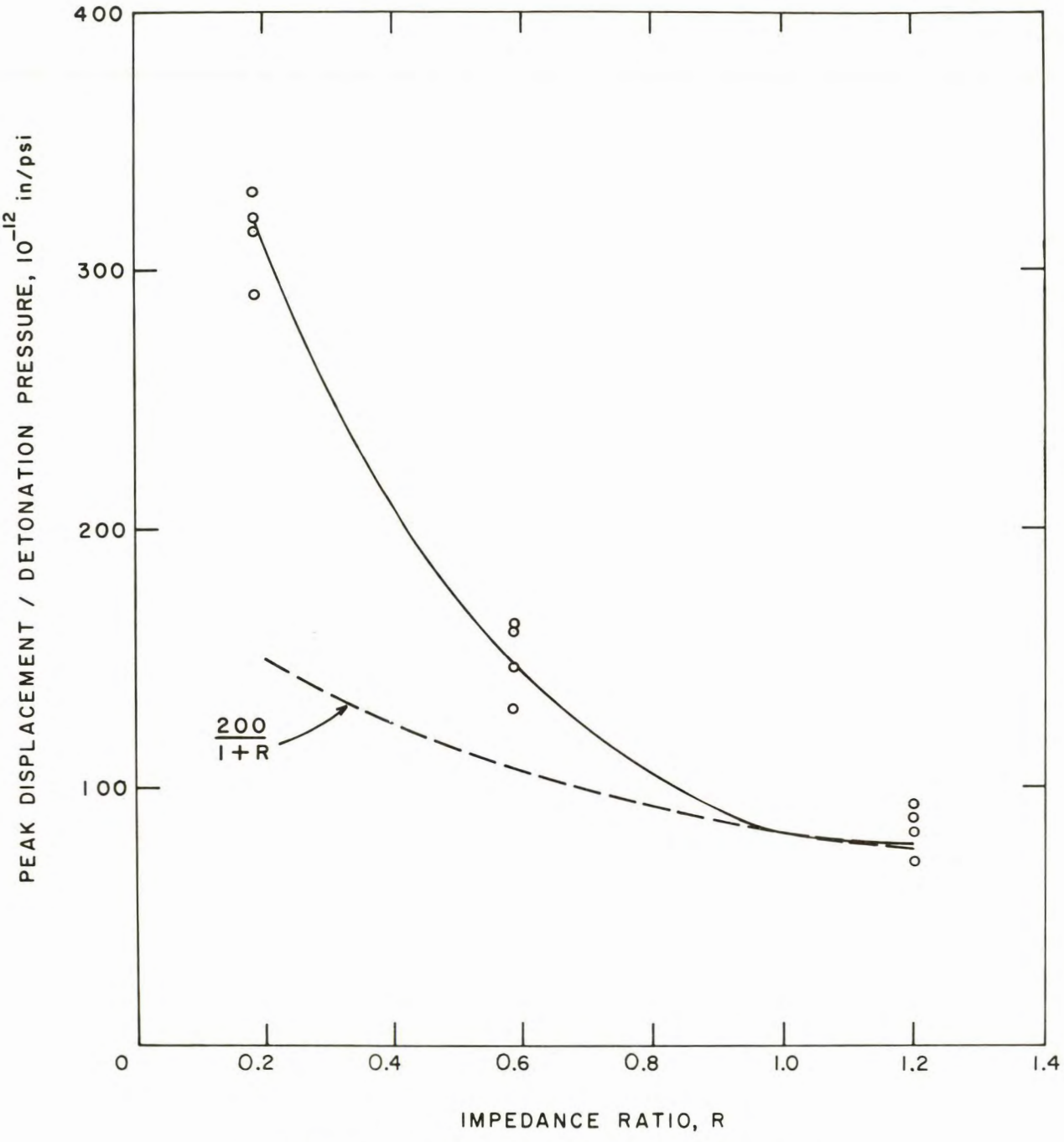

FIGURE 12. - Impedance Effect for Peak Displacement.

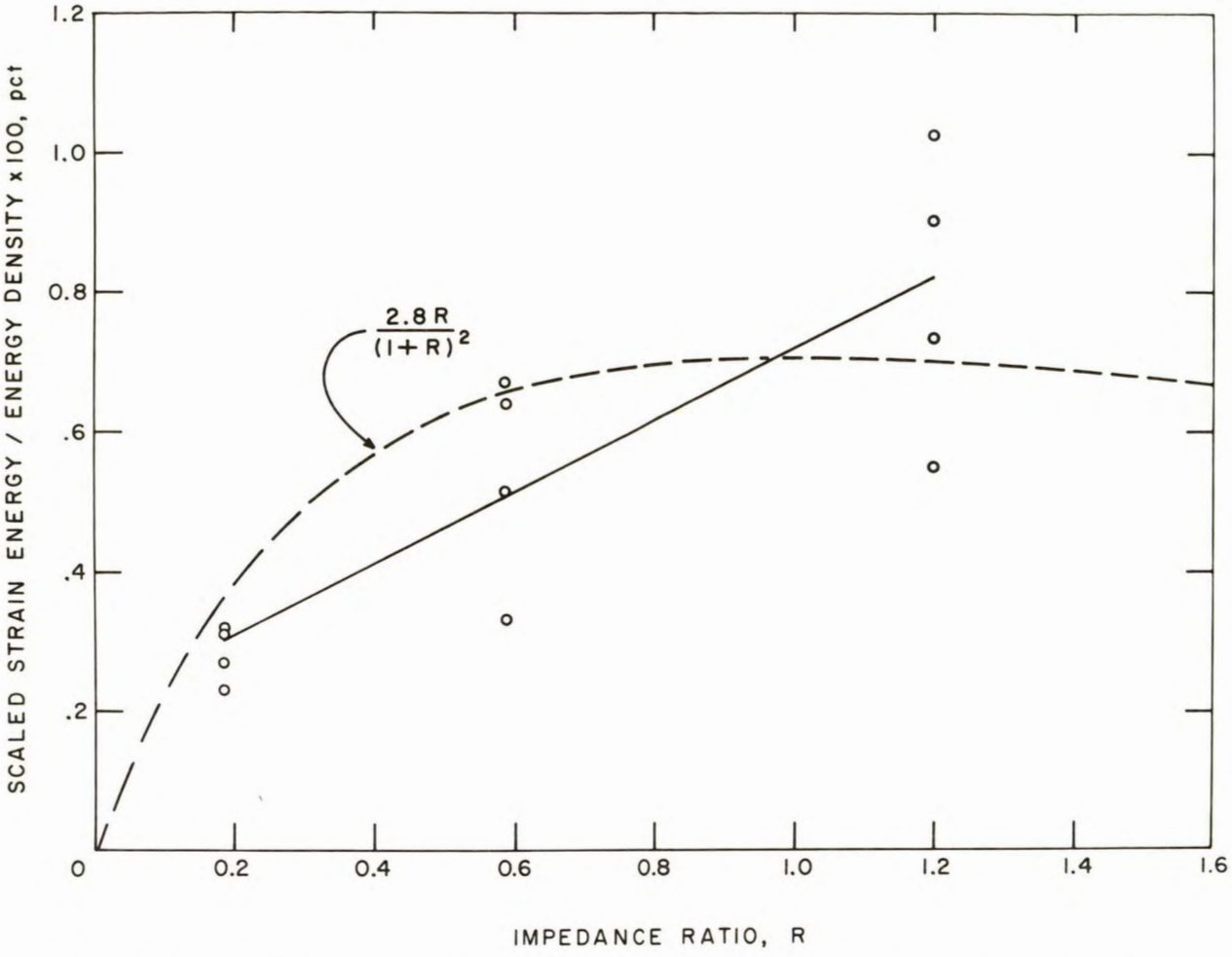

FIGURE 13. - Relative Energy Transfer as a Function of Characteristic Impedance Ratio.

Maximum Crater Dimensions

Figures 14, 15, and 16 are plots of scaled crater dimensions versus scaled charge depth where scaling is to the cube root of the charge volume. The curves through the data on these figures are second degree polynomials. Although both second and third degree polynomials were fitted to the data, statistical tests showed that the second degree equations adequately described the data.

Because of the scatter in figures 14, 15, and 16, estimates of crater dimensions from the least squares curves will have considerable error. However, it is apparent that the higher density charges generally produce larger crater dimensions at a given charge depth and continue cratering to greater depths.

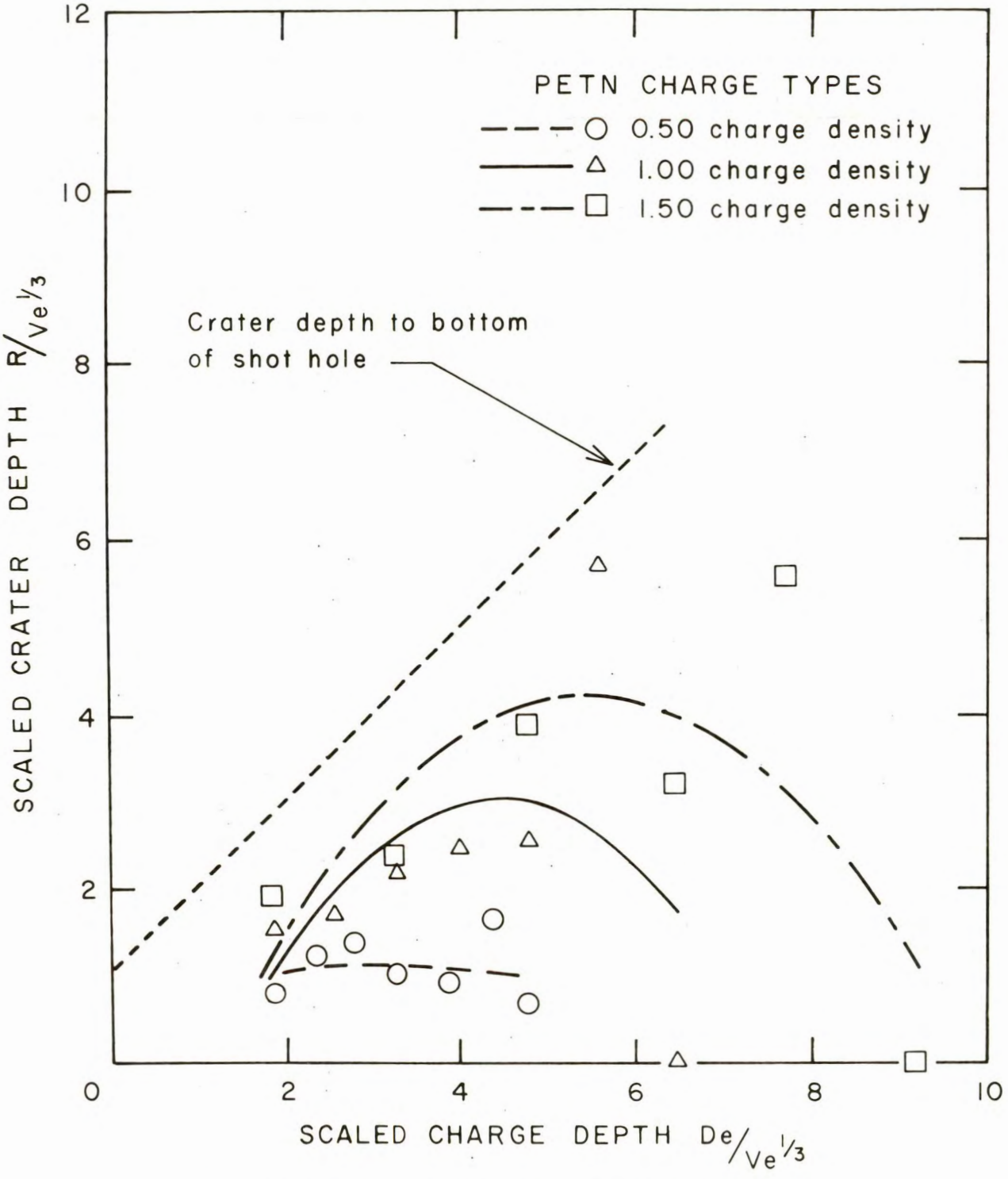

FIGURE 14. - Crater Depth as a Function of Charge Depth.

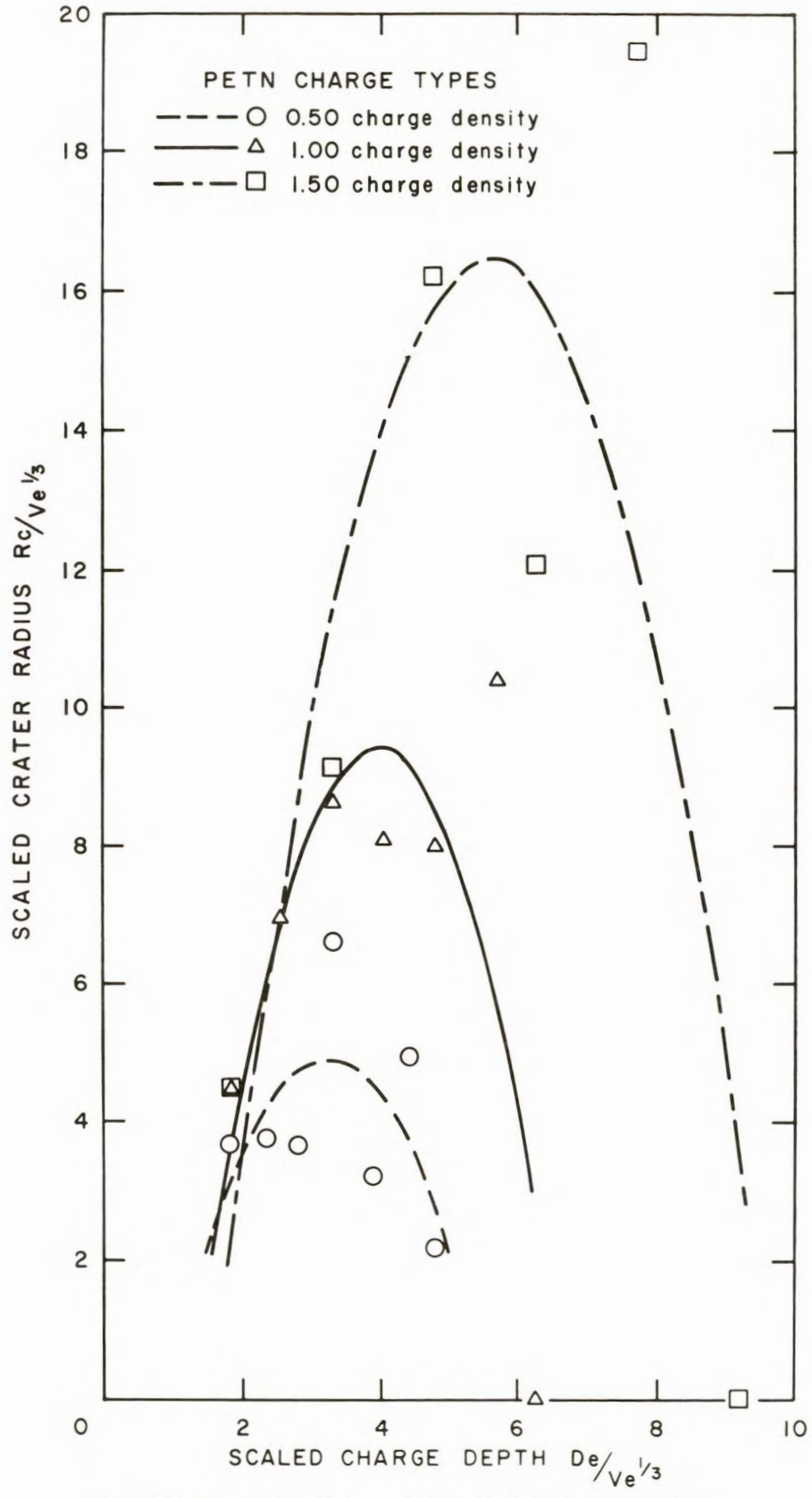

FIGURE 15. - Crater Radius as a Function of Charge Depth.

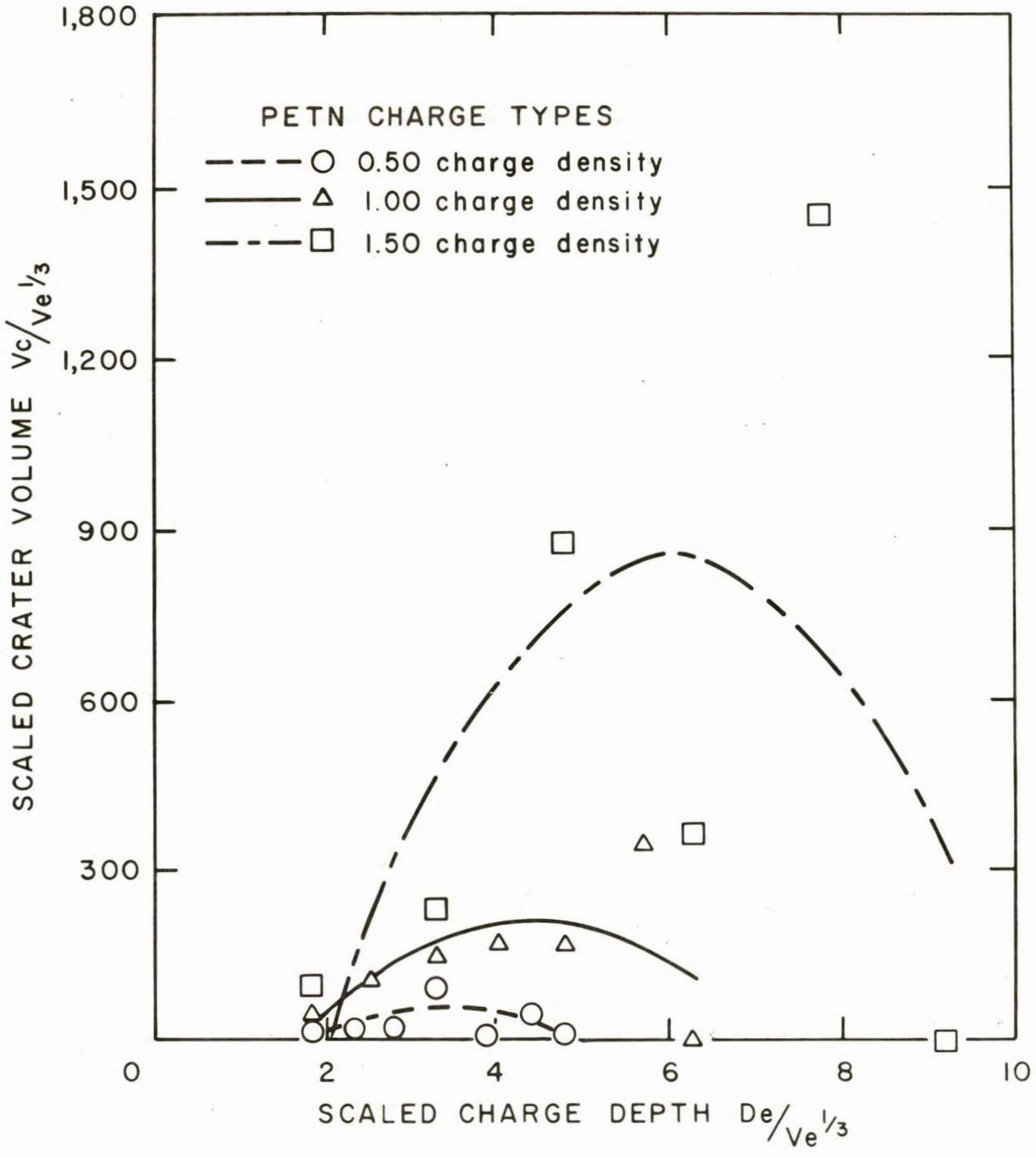

FIGURE 16. - Crater Volume as a Function of Charge Depth.

Table 7 is a summary comparing the relative properties of the PETN charges with displacement pulse parameters, strain energy, and optimum crater dimensions. In table 7 the values associated with the 1.0 specific gravity charge are given a value of 100 and the values for the other two explosive densities are scaled to it. Average values were used for the displacement pulse parameters and strain energy. The least squares fits of the crater data provided the optimum crater values listed in table 7.

TABLE 7. - Relative performance of PETN charges[1] [2]

Property	Relative value		
	ρ = 0.50	ρ = 1.00	ρ = 1.50
Explosive:			
Loading density	50	100	150
Detonation velocity	64	100	136
Detonation pressure	21	100	276
Detonation temperature	97	100	104
Specific energy	97	100	104
Energy density	49	100	156
Energy release rate	32	100	210
Displacement pulse:			
Peak displacement	44	100	154
Displacement duration	82	100	115
Displacement rise time	81	100	115
Displacement fall time	81	100	111
Displacement width	77	100	115
Strain energy	25	100	225
Crater:			
Maximum crater depth	41	100	140
Maximum crater radius	52	100	174
Maximum crater volume	30	100	410

[1] ρ = 1.00 taken as 100.

[2] Comparison is made on an equal volume basis at 80 percent coupling.

Table 7 shows that there is an approximate 1:1 correlation between maximum crater depth or maximum crater radius and explosive loading density or energy density. Crater volume is not directly proportional to any of the explosive properties with the possible exception of detonation pressure. The approximate direct correlation between peak displacement and crater depth or crater radius suggests that peak displacement measurements are a good indicator of explosive effectiveness in cratering.

Although there are increases in optimum crater dimensions associated with increases in all of the explosive properties listed in table 7, the percentage changes in detonation temperature and specific energy are so small that for practical applications these properties cannot be considered good indicators of explosive performance. Loading density cannot be used to rate all explosives because for some explosives such as straight gelatins and ammonia gelatins the energy density does not increase as the loading density increases. The detonation velocity, detonation pressure, energy density, and energy release rate then are the best indicators of explosive performance.

CONCLUSIONS

Changes in the properties of an explosive can have a pronounced effect on the ability of the explosive to generate stress waves and to form craters. In this laboratory experiment with constant-volume PETN charges, the amplitude and duration of free-surface displacement pulses and the strain energy generated in a cement-mortar were significantly increased by increasing the explosive loading density. Crater tests in cement-mortar with these same charges showed that maximum crater dimensions also were significantly increased by increasing the loading density.

Increasing the loading density of the PETN charges increased the detonation velocity, detonation pressure, detonation temperature, specific energy (ft lb/lb), energy density (ft lb/ft^3), and energy release rate. The best indicators of explosive performance were found to be loading density, detonation velocity, detonation pressure, energy density, and energy release rate. However, the use of loading density to rate explosives can be misleading because for some commercial gelatin-type explosives the energy density decreases with increasing loading density (7, p. 17).

In this laboratory experiment it was found that the maximum linear crater dimensions (crater depth and crater radius) were approximately directly proportional to the explosive loading density or energy density. Maximum crater volume was most nearly directly proportional to explosive detonation pressure.

The peak amplitudes of the free-surface displacement pulses were approximately directly proportional to the linear crater dimensions confirming that peak amplitude measurements can be used to evaluate explosive performance.

It was found that simple acoustic relationships involving impedance ratios could not be used to predict the peak displacement or strain energy generated in the cement-mortar by the explosive. The data suggest that energy transmission from an explosive to a rock continues to be increasingly more efficient as the impedance of the explosive matches and then exceeds that of the rock.

REFERENCES

1. Ash, Richard L. The Mechanics of Rock Breakage. Pit and Quarry, v. 56, No. 8, August 1963, pp. 98-100 (pt. 1); v. 56, No. 9, September 1963, pp. 118-123 (pt. 2); v. 56, No. 10, October 1963, pp. 109-111 (pt. 3); v. 56, No. 11, November 1963, pp. 114-118 (pt. 4).

2. Atchison, Thomas C., and Joseph M. Pugliese. Comparative Studies of Explosives in Granite. Second Series of Tests. BuMines Rept. of Inv. 6434, 1964, 26 pp.

3. Atchison, T. C., and W. W. Tournay. Comparative Studies of Explosives in Granite. BuMines Rept. of Inv. 5509, 1959, 28 pp.

4. Brown, F. W. Determination of Basic Performance Properties of Blasting Explosives. Colorado Sch. Mines Quart., v. 51, No. 3, 1956, pp. 169-188.

5. Bur, Thomas R., Lyle W. Colburn, Harry R. Nicholls, and Thomas E. Slykhouse. Comparison of Two Methods for Studying Relative Performance of Explosives in Rock. BuMines Rept. of Inv. 6888, 1967, 40 pp.

6. Cook, M. A. The Science of High Explosives. ACS Monograph 139, Reinhold Pub. Corp., New York, 1958, 440 pp.

7. Dick, Richard A. Factors in Selecting and Applying Commercial Explosives and Blasting Agents. BuMines Inf. Circ. 8405, 1968, 30 pp.

8. Department of the Army. Military Explosives Technical Manual. TM9-1910, 1955, p. 41.

9. Dunkle, Cyrus G., and others. Detonation Phenomena, Compilation of SYLLABI, Picatinny Arsenal. Stevens Inst. Technol. Graduate Course, 1957, 409 pp.; DDC, AD 202170.

10. Duvall, W. I., and T. C. Atchison. Rock Breakage by Explosives. BuMines Rept. of Inv. 5356, 1957, 52 pp.

11. Duvall, W. I., T. C. Atchison, and D. E. Fogelson. Empirical Approach to Problems in Blasting Research. Proc., 8th Symp. Rock Mechanics, Univ. Minnesota, AIME, New York, 1967, pp. 500-523.

12. E. I. du Pont de Nemours and Co., Inc. Blaster's Handbook. 15th ed., 1966.

13. Eyring, H., R. E. Powell, G. H. Duffy, and R. B. Parlin. The Stability of Detonation. Chem. Rev., v. 45, 1949, pp. 69-181.

14. Fairhurst, C. Laboratory Measurement of Some Physical Properties of Rock. Proc., 4th Symp. Rock Mechanics, Pennsylvania State Univ., Mineral Industries Exp. Sta. Bull., 1961, pp. 105-118.

15. Fogelson, D. E., D. V. D'Andrea, and R. L. Fischer. Effects of Decoupling and Stemming on Explosion-Generated Pulses in Mortar: A Laboratory Study. BuMines Rept. of Inv. 6679, 1965, 18 pp.

16. Fogelson, David E., Wilbur I. Duvall, and Thomas C. Atchison. Strain Energy in Explosion-Generated Strain Pulses. BuMines Rept. of Inv. 5514, 1959, p. 3.

17. Grant, Bruce F., Wilbur I. Duvall, Leonard Obert, R. L. Rough, and T. C. Atchison. Use of Explosives in Oil and Gas Wells--1949 Test Results. BuMines Rept. of Inv. 4714, 1950, 29 pp.

18. Hubbs, John C. The New Pulse. 8th Ann. Nat. Meeting of the Precision Measurements Assoc., Los Angeles, Calif., September 1965 (rev. January 1966), 23 pp.

19. Jacobs, S. J. Recent Advances in Condensed Media Detonations. ARS J., v. 30, No. 2, February 1960, pp. 151-158.

20. Johnson, J. Burlin. Small-Scale Blasting in Mortar. BuMines Rept. of Inv. 6012, 1962, 22 pp.

21. Johnson, J. Burlin, and R. L. Fischer. Effects of Mechanical Properties of Material on Cratering: A Laboratory Study. BuMines Rept. of Inv. 6188, 1963, 24 pp.

22. Langefors, Ulf, and B. A. Kihlstrom. The Modern Technique of Rock Blasting. John Wiley & Sons, Inc., New York, 2d ed., 1967, 405 pp.

23. MacDougal, D. P., and R. Messerly. The Effect of Particle Size on the Detonation Velocity of Ammonium Picrate. Nat. Res. Comm., Office of Scientific Research and Development, OSRD Rept. 1755, 1943, 10 pp.

24. Monroe, C. E., and J. E. Tiffany. Physical Testing of Explosives. BuMines Bull. 346, 1931, 148 pp.

25. Nicholls, Harry R., and Wilbur I. Duvall. Effect of Characteristic Impedance on Explosion-Generated Strain Pulses in Rock. Proc., 5th Symp. Rock Mechanics, Univ. Minnesota, Pergamon Press, New York, 1964, pp. 331-346.

26. _____. Effect of Charge Diameter on Explosive Performance. BuMines Rept. of Inv. 6806, 1966, 22 pp.

27. Obert, Leonard, and Wilbur I. Duvall. A Gage and Recording Equipment for Measuring Dynamic Strain in Rock. BuMines Rept. of Inv. 4581, 1949, 11 pp.

28. Ostle, B. Statistics in Research. Iowa State College Press, Ames, Iowa, 1954, pp. 138-142.

29. Sadwin, L. D., C. M. Cooley, S. J. Porter, and R. H. Stressau. Underwater Evaluation of the Performance of Explosives. Proc., Internat. Symp. Mining Research, Pergamon Press, New York, v. 1, 1962, pp. 125-134.

30. Sadwin, L. D., and W. I. Duvall. A Comparison of Explosives by Cratering and Other Methods. Trans. AIME, v. 232, 1965, pp. 110-115.

31. Sadwin, L. D., R. H. Stressau, S. J. Porter, and J. Savitt. Nonideal Detonation of Ammonium Nitrate-Fuel Mixtures. Proc., 3d Symp. Detonation, Princeton, N.J., September 1960, pp. 309-325.

32. Starfield, A. M., and J. M. Pugliese. Compression Waves Generated in Rock by Cylindrical Explosive Charges: A Comparison Between a Computer Model and Field Measurements. Internat. J. Rock Mech. and Min. Sci., v. 5, No. 1, January 1968, pp. 65-77.

33. Taylor, J. Detonation in Condensed Explosives. Oxford Univ. Press, London, 1952, 196 pp.

INT.-BU.OF MINES,PGH.,PA. 14987